2017-01-04

Interplay between stress permutations and overpressure to cause strike-slip faulting during tectonic inversion

Peacock, DCP

http://hdl.handle.net/10026.1/8668
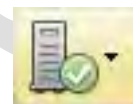
WILEY
Online Proofing System Instructions

The Wiley Online Proofing System allows authors and proof reviewers to review PDF proofs, mark corrections, respond to queries, upload replacement figures, and submit these changes directly from the PDF proof from the locally saved file or while viewing it in your web browser.

1. For the best experience reviewing your proof in the Wiley Online Proofing System please ensure you are connected to the internet. This will allow the PDF proof to connect to the central Wiley Online Proofing System server. If you are connected to the Wiley Online Proofing System server you should see the icon with a green check mark above in the yellow banner.

Connected   Disconnected

2. Please review the article proof on the following pages and mark any corrections, changes, and query responses using the Annotation Tools outlined on the next 2 pages.

3. To save your proof corrections, click the "Publish Comments" button appearing above in the yellow banner. Publishing your comments saves your corrections to the Wiley Online Proofing System server. Corrections don't have to be marked in one sitting, you can publish corrections and log back in at a later time to add more before you click the "Complete Proof Review" button below.
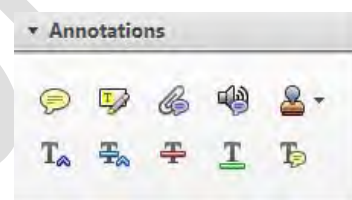
4. If you need to supply additional or replacement files <u>bigger</u> than 5 Megabytes (MB) do not attach them directly to the PDF Proof, please click the "Upload Files" button to upload files:

5. When your proof review is complete and you are ready to submit corrections to the publisher, please click the "Complete Proof Review" button below:

IMPORTANT: <u>Do not click the "Complete Proof Review" button without replying to all author queries found on the last page of your proof</u>. Incomplete proof reviews will cause a delay in publication.

IMPORTANT: Once you click "Complete Proof Review" you will not be able to publish further corrections.

WILEY

Once you have Acrobat Reader open on your computer, click on the Comment tab at the right of the toolbar:
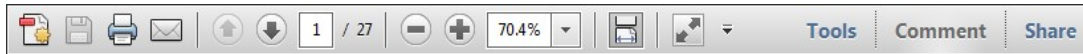
This will open up a panel down the right side of the document. The majority of tools you will use for annotating your proof will be in the Annotations section, pictured opposite. We've picked out some of these tools below:
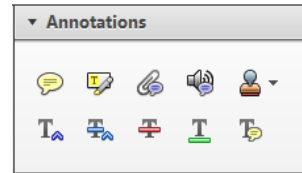
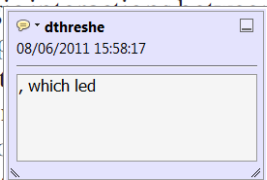### 1. Replace (Ins) Tool – for replacing text.

Strikes a line through text and opens up a text box where replacement text can be entered.

How to use it

- Highlight a word or sentence.
- Click on the Replace (Ins) icon in the Annotations section.
- Type the replacement text into the blue box that appears.

ndard framework for the analysis of m
icy. Nevertheless, it also led to exoge
ole of strategi interaction haten fi
nber of comp   to
is that the st   of
nain compo   be
level, are exc   nd
important works on entry by Onro
M henceforth)[1] we open the 'black h

dthreshe
08/06/2011 15:58:17

, which led

---

2. Strikethrough (Del) Tool – for deleting text.

Strikes a red line through text that is to be deleted.

How to use it

- Highlight a word or sentence.
- Click on the Strikethrough (Del) icon in the Annotations section.

there is no room for extra profits ar
ups are zero and the number of
ket) values are not determined by
Blanchard and Kiyotaki (1987),
rfect competition in general equilil
ts of aggregate demand and supply
lassical framework assuming mono
een an exogenous number of firms

---

3. Add note to text Tool – for highlighting a section to be changed to bold or italic.

Highlights text in yellow and opens up a text box where comments can be entered.

How to use it

- Highlight the relevant section of text.
- Click on the Add note to text icon in the Annotations section.
- Type instruction on what should be changed regarding the text into the yellow box that appears.

namic responses of mark ups
ent with the VAR evidence

sation   ith
y Ma   ell
and   led
on n   ber
to a   on
stent also with the demand-

dthreshe
08/06/2011 15:31:38

---

4. Add sticky note Tool – for making notes at specific points in the text.

Marks a point in the proof where a comment needs to be highlighted.

How to use it

- Click on the Add sticky note icon in the Annotations section.
- Click at the point in the proof where the comment should be inserted.
- Type the comment into the yellow box that appears.

land and supply shocks. Most of
amin   eti
numbe   iff
dard fr   sis
icy. Nev   o
ole of st   wo
ber of competitors and the imp
is that the structure of the secto

dthreshe
08/06/2011 15:18:08

5. Attach File Tool – for inserting large amounts of text or replacement figures.

Inserts an icon linking to the attached file in the appropriate place in the text.

How to use it

- Click on the Attach File icon in the Annotations section.
- Click on the proof to where you'd like the attached file to be linked.
- Select the file to be attached from your computer or network.
- Select the colour and type of icon that will appear in the proof. Click OK.
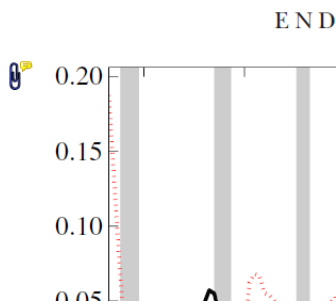
6. Drawing Markups Tools – for drawing shapes, lines and freeform annotations on proofs and commenting on these marks.

Allows shapes, lines and freeform annotations to be drawn on proofs and for comment to be made on these marks.
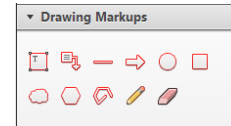
How to use it

- Click on one of the shapes in the Drawing Markups section.
- Click on the proof at the relevant point and draw the selected shape with the cursor.
- To add a comment to the drawn shape, move the cursor over the shape until an arrowhead appears.
- Double click on the shape and type any text in the red box that appears.
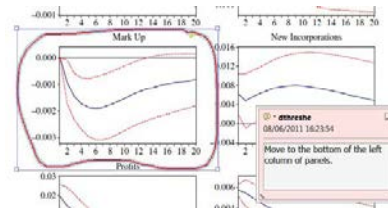
Interplay between stress permutations and overpressure to cause strike-slip faulting during tectonic inversion

David C. P. Peacock,[1] 🆔 Enrico Tavarnelli[2] and Mark W. Anderson[3]

[1]Department of Earth Science, University of Bergen, Allégaten 41, Bergen 5007, Norway; [2]Dipartimento di Scienze Fisiche della Terra e dell'Ambiente, Università di Siena, Siena I-53100, Italy; [3]School of Geography, Earth and Environmental Sciences, University of Plymouth, Plymouth PL4 8AA, UK

ABSTRACT

Field data from an orogenic foreland and an orogenic belt (the Mesozoic rocks of southern England and the Umbria-Marche Apennines of Italy respectively) indicate the following. Firstly, stress evolution during the tectonic cycle, between maximum compressive stress (σ_1) being vertical during extension and least compressive stress (σ_3) being vertical during contraction, can involve phases when the intermediate compressive stress (σ_2) is vertical, promoting strike-slip deformation. Secondly, variations in the relative magnitudes of the stress axes are caused by variations in overburden and tectonic forces. Thirdly, overpressure can develop because of

compaction during burial, and, as overburden is reduced during uplift and erosion, the vertical stress (σ_V) reduces but fluid pressure (P_f) remains approximately constant. Brittle deformation, including transient strike-slip faults, reverse-reactivated normal faults and normal-reactivated thrusts, is preferentially developed in overpressured areas because high P_f promotes faulting.

Terra Nova, 00: 1–10, 2016

Introduction

Interpretations of stress orientations, fluid pressures (P_f) and deformation chronologies are keys to most structural analyses. Here, we link the changes in the magnitudes of stress axes with related changes in P_f to understand a common phase of strike-slip deformation between periods of regional extension and regional contraction. Many regions show both extensional and contractional events, with structures reactivating or overprinting each other during *tectonic inversion* (e.g. Butler *et al.*, 2006). *Positive inversion* is the change from extension to contraction (e.g. Williams *et al.*, 1989), while *negative inversion* is the change from contraction to extension (e.g. Lake and Karner, 1987). Inversion implies a stress evolution in which there is interchange between σ_3 being vertical to cause vertical thickening, and σ_1 being vertical to cause vertical thinning.

Strike-slip faults develop in a variety of tectonic systems when $\sigma_2 = \sigma_V$ and have been reported to form during the transition from orogenesis to

orogenic collapse (e.g. Dewey, 1969; Lavecchia and Pialli, 1981) and after basin development but ahead of subsequent contractional events (e.g. Vandycke, 2002). Angelier *et al.* (1985) define *stress permutation* as switches between the principal stress axes, with either σ_1 and σ_2 swapping over, or σ_2 and σ_3 swapping over. Stress permutation has been described in different tectonic regimes, including contractional (Tranos, 2013), strike-slip (Van Noten *et al.*, 2013), extensional (Sue *et al.*, 2014), rifts (Plateaux *et al.*, 2012), passive margins (Mazabraud *et al.*, 2013) and shield volcanoes (Chaput *et al.*, 2014). We show that changes between vertical σ_1 and vertical σ_3 typically involve a phase in which $\sigma_2 = \sigma_V$, which tends to cause strike-slip faulting.

High P_f is common in sedimentary basins (e.g. Swarbrick *et al.*, 2002), and *overpressure* refers to the condition in which P_f is greater than the hydrostatic pressure of an equivalent free column of water (e.g. Bowers, 2002; figs 4 and 5; Sibson, 2004; fig. 1). Maintenance of high P_f typically requires a seal lithology. Hubbert and Rubey (1959) show that thrust sheets slide on layers of overpressured fluids that reduce friction. Overpressure can develop as sediments are compacted during burial, as thermal expansion occurs and as

hydrocarbons are generated (e.g. Cobbold *et al.*, 2004; Lahann and Swarbrick, 2011). Overpressure can also develop during uplift and erosion events, as overburden is reduced but P_f is maintained (e.g. Doré and Jensen, 1996; Corcoran and Doré, 2002).

The aim of this paper was to show that the interplay between stress permutations and overpressure, generated during subsidence and uplift, helps explain the processes acting during inversion, especially the development of strike-slip faults between extensional and contractional events. The example of structures in southern England is used because the area was affected by Alpine contraction but did not experience significant crustal shortening and thickening, so the inversion structures are well-preserved. Examples from the Apennines of Italy are presented to show that these phases of strike-slip faulting can be recognised in orogenic belts.

Mesozoic rocks of southern England

Structures in the Liassic limestones and shales between Lilstock and East Quantoxhead, Somerset (Fig. 1), demonstrate Mesozoic basin development and Tertiary (Alpine) basin inversion (e.g. Dart *et al.*, 1995).

Correspondence: David C. P. Peacock, Department of Earth Science, University of Bergen, Allégaten 41, Bergen 5007, Norway. Tel.: +47 945101968; e-mail: hermangedge@gmail.com

Several palaeostress orientation analyses of the Bristol Channel Basin have been published (e.g. Peacock and Sanderson, 1992; Dart *et al.*, 1995; Nemčok *et al.*, 1995; Glen *et al.*, 2005). The deformation history is as follows:

1 Normal faults striking ˜095° and related E–W-striking calcite veins and gentle folds (Figs 1b, 2a, and 3a) were caused by ˜N–S extension during Mesozoic development of the Bristol Channel Basin (e.g. Nemčok *et al.*, 1995). The normal faults have displacements of up to hundreds of metres (Whittaker and Green, 1983). The Liassic limestones and shales in Somerset are unlikely to have been buried to a depth of < 2 km, based on the thicknesses of the overlying sequence in the region.

2 Evidence for sinistral shear followed by dextral reactivation of some 095°–striking normal faults (Peacock and Sanderson, 1999) includes the steepening of beds in relay ramps (Fig. 2b) and shear around some normal faults (Fig. 3b). This suggests σ_1 was orientated ˜NW–SE. Hibsch *et al.* (1995) describe Upper Jurassic to Early Cretaceous E–W to WNW–ESE transtension elsewhere in England, while Vandycke and Bergerat (2001) describe strike-slip faulting, with σ_1 orientated NNE–SSW to N–S, in the Cretaceous Chalk of the Isle of Wight.

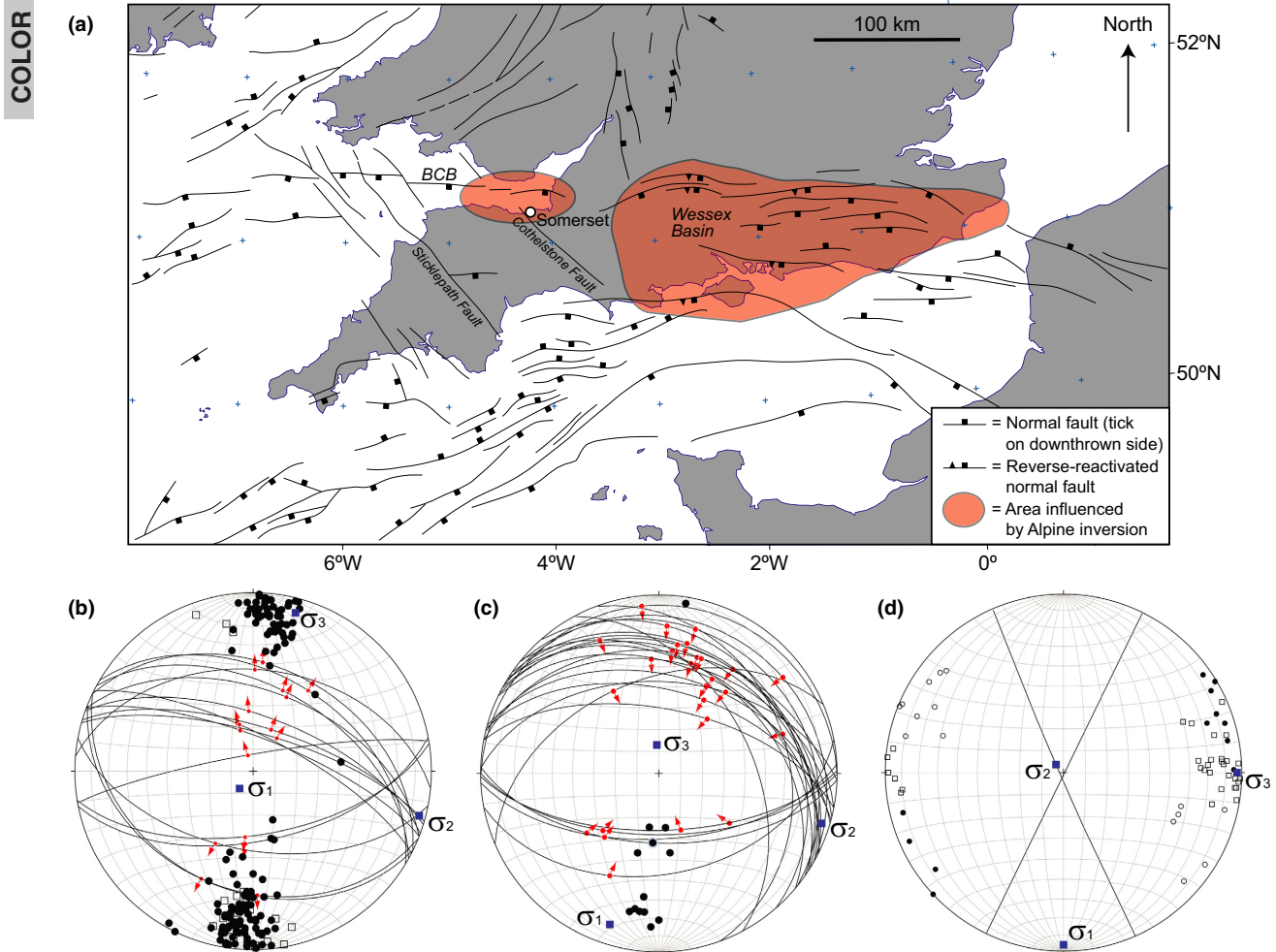3 The Tertiary deformation that produced the Alpine Mountains further south and southeast in

Fig. 1 (a) Map of southern England, showing the major structures (based on Petroleum Exploration Society of Great Britain, 2000). The location of the Somerset field area (51.1797°N, 3.2158°W) is shown. (b) Stereogram for normal faults. Unstriated fault planes are plotted as poles (filled circles), while striated fault planes are plotted as great circles with slip indicators also plotted (in red). σ_1 plunges 80° towards 218°, σ_2 plunges 4° towards 105° and σ_3 plunges 9° towards 015°. (c) Stereogram for thrusts and reverse-reactivated faults. Unstriated fault planes are plotted as poles (filled circles), while striated fault planes are plotted as great circles with slip indicators also plotted (in red). σ_1 plunges 12° towards 198°, σ_2 plunges 5° towards 107° and σ_3 plunges 77° towards 356°. (d) Stereogram for strike-slip faults. Poles to dextral faults are filled circles, and poles to sinistral faults are unfilled circles. The two great circles shown for the strike-slip are the mean orientations for each set. Veins are plotted as unfilled squares. σ_1 plunges 4° towards 180°, σ_2 plunges 85° towards 317° and σ_3 plunges 3° towards 090°.
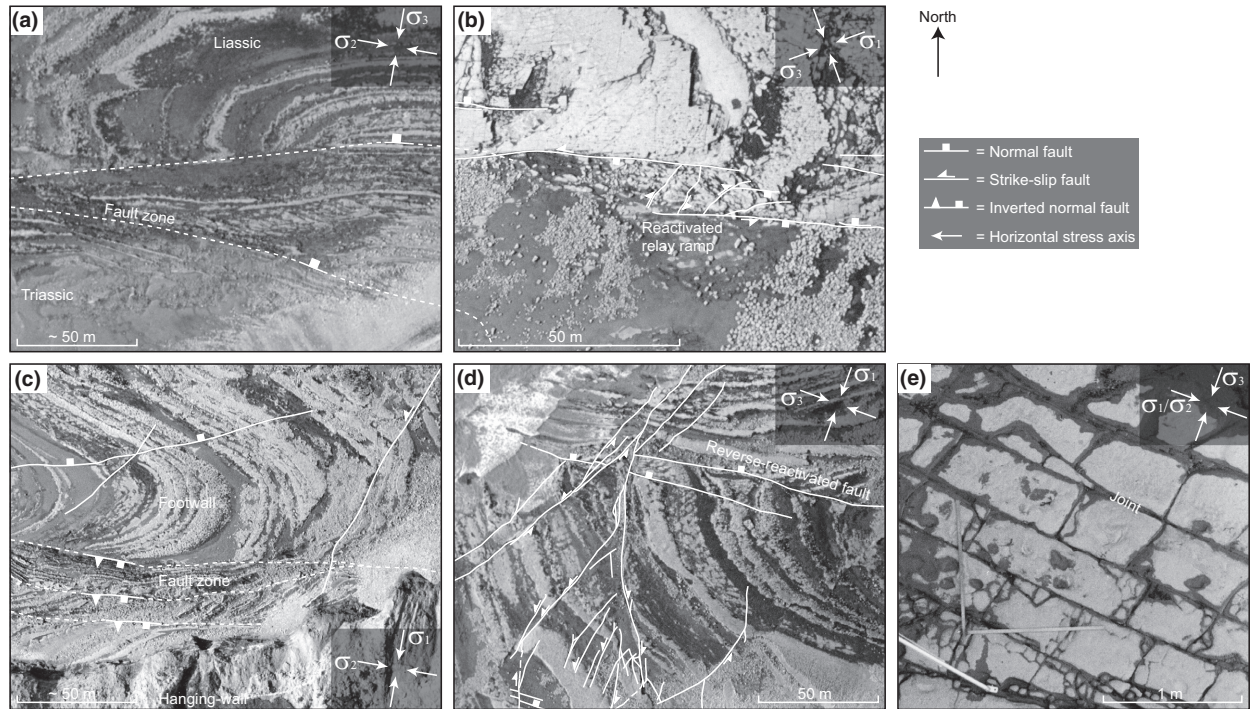
Fig. 2 Aerial photographs of the beach in Somerset, with the inferred stress directions during formation of the structures shown. (a) Normal fault displacing Triassic marls against Liassic limestones and shales. (b) Relay ramp between stepping normal faults, reactivated as a sinistral strike-slip fault, causing steepening of the relay ramp. (c) The East Quantoxhead Fault, which shows evidence for reverse-reactivation (e.g. Peacock and Sanderson, 1999). (d) Strike-slip faults displacing reverse-reactivated normal faults. (e) Photograph taken from a height of ~4 m, showing joints on a Liassic limestone bedding plane. The master joints strike ~ NW–SE.
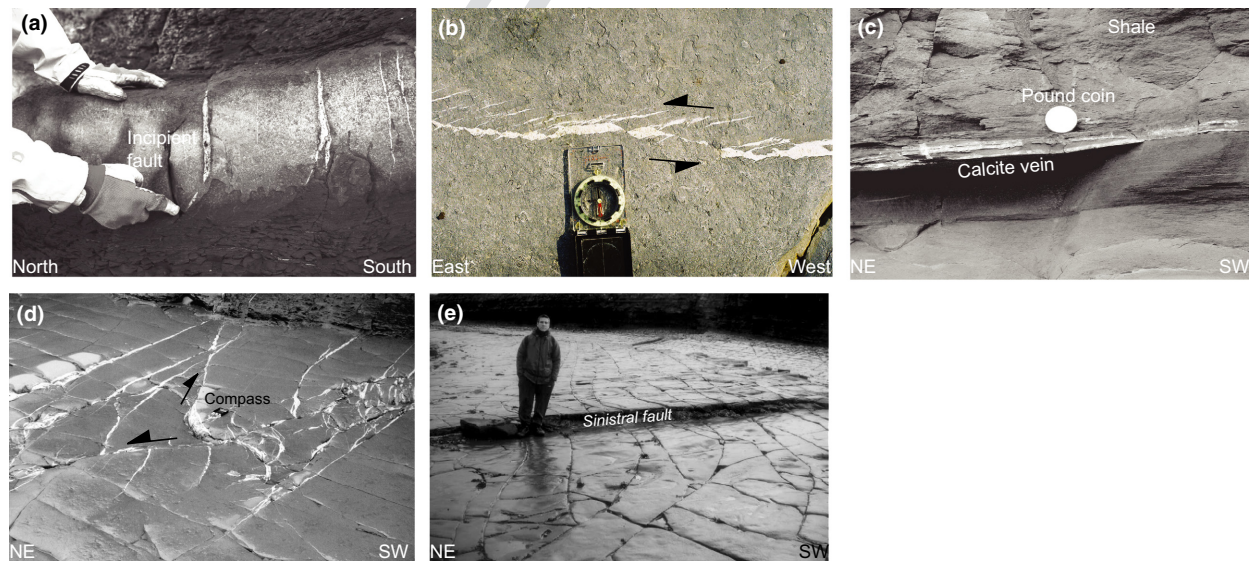

Fig. 3 Structures in the Liassic rocks on the Somerset coast, with veins and joints being evidence for $P_f > \sigma_h$ during each deformation phase. (a) E–W-striking calcite veins, with one showing some vertical displacement (i.e. the initiation of normal faulting). (b) E–W-striking sinistral pull-aparts, within 1 m of the reactivated normal fault zone shown in Fig. 2(b), east of Lilstock. (c) Bed-parallel calcite vein in shale, indicating overpressure during inversion. (d) A sinistral strike-slip fault with smaller dextral faults in the wall rocks. N–S-striking calcite veins occur along and around the faults. (e) Joints that curve into, and therefore post-date, a sinistral strike-slip fault.
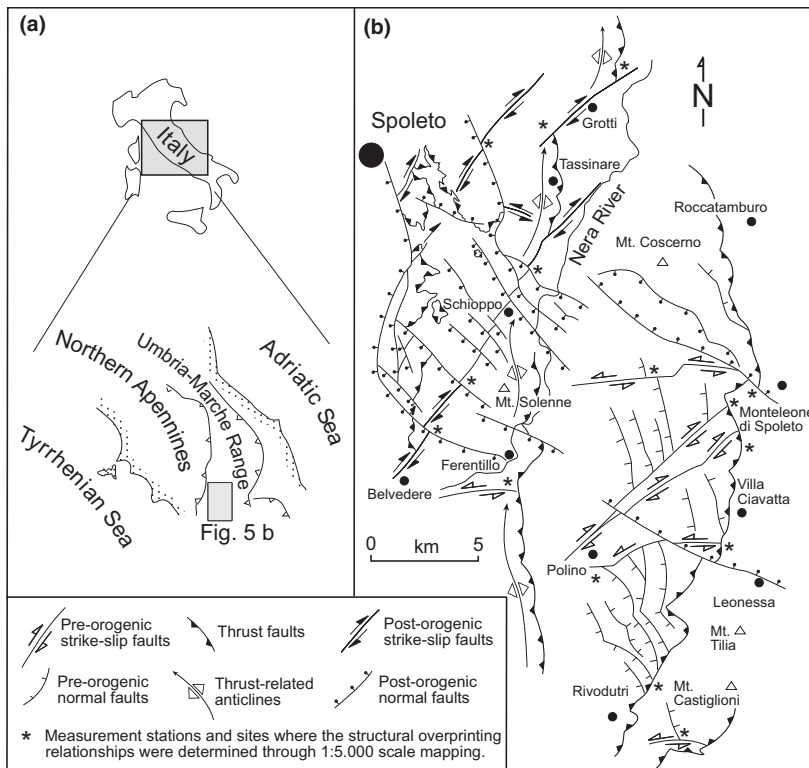
Fig. 4 (a) Tectonic map of the Northern Apennines, showing the location of the Umbria-Marche Range. (b) Structural map of the area SE of Spoleto (location in Fig. 4a), based on field mapping carried out at a scale of 1:25000.

Europe is commonly marked in southern England by the inversion of Mesozoic and older structures (e.g. Underhill and Patterson, 1998) (Fig. 1). N–S contraction is illustrated by N–S-striking calcite veins, E–W-striking thrusts, E–W-striking folds (including crenulation cleavage) and inversion of some 095°-striking normal faults (Fig. 1c; Peacock and Sanderson, 1999). Contraction did not involve a significant increase in overburden, for example, by thrust stacking.

4 The reverse-reactivated normal faults are cut by strike-slip faults conjugate about ˜010° and with displacements of up to hundreds of metres (e.g. Whittaker, 1972; Dart *et al.*, 1995; Figs 1a,d and 2d). The inversion did not involve significant crustal thickening, so the transition between $\sigma_3 = \sigma_V$ and $\sigma_2 = \sigma_V$ may have been caused by a decrease in σ_h, possibly related to the Palaeogene opening of the Atlantic Ocean.

5 The post-faulting joints (Figs 2e and 3e; Peacock, 2001) may represent the reduction of Alpine stresses (Rawnsley *et al.*, 1998).

Evidence for $P_f > \sigma_3$ during each event includes calcite veins and joints (Fig. 3).

The Umbria-Marche Apennines

The Umbria-Marche range is an arcuate mountain belt in the outer zones of the Northern Apennines, Italy (Fig. 4a). The sequence of Mesozoic–Tertiary marine sediments was deposited mainly under pelagic conditions on the passive margin of the Adria continental microplate. Analysis was carried out over a ~450 km^2 area in the Nera River valley (Fig. 4b). The region is dominated by Upper Messinian thrusts and folds (Calamita *et al.*, 1994). Thrusting occurred at depths of 2–3 km under non-metamorphic conditions (Rusciadelli *et al.*, 2005; Tesei *et al.*, 2013). Fold–thrust structures are overprinted by late-orogenic,

Upper Miocene–Lower Pliocene conjugate strike-slip faults and by post-orogenic, Upper Pliocene–Quaternary normal faults. Pre-orogenic fault systems are, however, recognised (Decandia and Giannini, 1977; Decandia, 1982; Barchi, 1991; Tavarnelli, 1996; Tavarnelli and Peacock, 1999; Scisciani *et al.*, 2001), thus making it possible to determine the deformation history of the region (Tavarnelli, 1999; Pace *et al.*, 2016). Five phases of deformation are identified:

1 Syn-sedimentary normal faults developed during Late Triassic continental rifting and subsequent opening of the Tethys Ocean during the Jurassic, when the Adria continental margin drifted away from Europe (e.g. Alvarez, 1990). Extension also occurred in Umbria-Marche during the Late Cretaceous–Early Tertiary (Decandia, 1982). Some extension continued up to the Late Tertiary, immediately prior to the onset of orogenesis (Tavarnelli and Peacock, 1999; Scisciani *et al.*, 2001). Mesozoic and early Tertiary extension is marked by both normal faults and sub-vertical veins, with bed-parallel stylolites also common. These structures indicate that $\sigma_1 > P_f > \sigma_3$ (Fig. 5a).

2 A hitherto unrecognised episode of strike-slip fault development occurred between pre-orogenic extension and orogenic contraction. Satolli *et al.* (2014) consider these strike-slip faults to be related to transpression and strain partitioning along oblique thrust ramps. A set of conjugate strike-slip faults occurs east of the Nera River, where post-orogenic extension was mild, making it possible to reconstruct the fold-and-thrust geometry in detail and hence to characterise pre-orogenic structures. The oldest recognised structures, as described above, are NNW–SSE-trending normal faults (Figs 4b and 6a). These structures are overprinted by conjugate strike-slip faults. The main faults are exposed for ˜10 km between Polino and Monteleone di Spoleto (Fig. 4b) and have dextral kinematics with a mean 041° slip direction (Fig. 6b). Conjugate

faults occur between Polino and Villa Ciavatta, with a mean 079° sinistral slip direction (Figs 4b and 6b). Other strike-slip faults in this conjugate system occur between Monte Solenne and Monteleone di Spoleto, north-east of Rivodutri and south of Ferentillo (Fig. 4b). Most of these strike-slip faults are overprinted and truncated by the gently W-dipping surface of the Monte Coscerno-Rivodutri thrust. The strike-slip faults therefore developed between pre-orogenic extension and orogenic thrusting (Fig. 5b).

3 The sedimentary sequence was detached from its basement along Upper Triassic evaporites during the Late Tertiary and was thickened by thrusting and folding (e.g.

Tavarnelli, 1997). The mean dip direction of the thrusts is towards WSW, with slickensides and shear fibres indicating hangingwall transport toward 069° (Fig. 6c). Thrust-related anticlines have a mean plunge of 18° towards 348° (Fig. 6c), indicating σ_1 was orientated ˜069°. Thrusting and bed-parallel veins indicate $P_f > \sigma_3 = \sigma_V$ (e.g. Hubbert and Rubey, 1959; Fig. 5c).

4 Thrusts and folds are overprinted by late-orogenic SW–NE-trending strike-slip faults (Decandia and Giannini, 1977; Decandia, 1982; Barchi, 1991), which produce a 10 m high scarp near Schioppo (Fig. 7a) that extends for >12 km between Belvedere and the Nera River south of Tassinare (Fig. 4b).

Other strike-slip faults occur near Spoleto and Grotti (Fig. 4b). Slickensides and shear fabrics along these faults consistently indicate dextral slip (Fig. 7b,c) with a mean 037° slip direction (Fig. 6d). A subordinate set of conjugate WSW–ENE-trending sinistral faults occurs (Fig. 4b), with a mean slip direction of 087°. These faults indicate $\sigma_2 = \sigma_V$ and that σ_1 was orientated ˜061° (Fig. 5d), and reveal a phase of stress perturbation (e.g. Decandia and Giannini, 1977; Lavecchia and Pialli, 1981; Marshak *et al.*, 1982; Calamita *et al.*, 1987; Alfonsi *et al.*, 1990; Barchi, 1991).

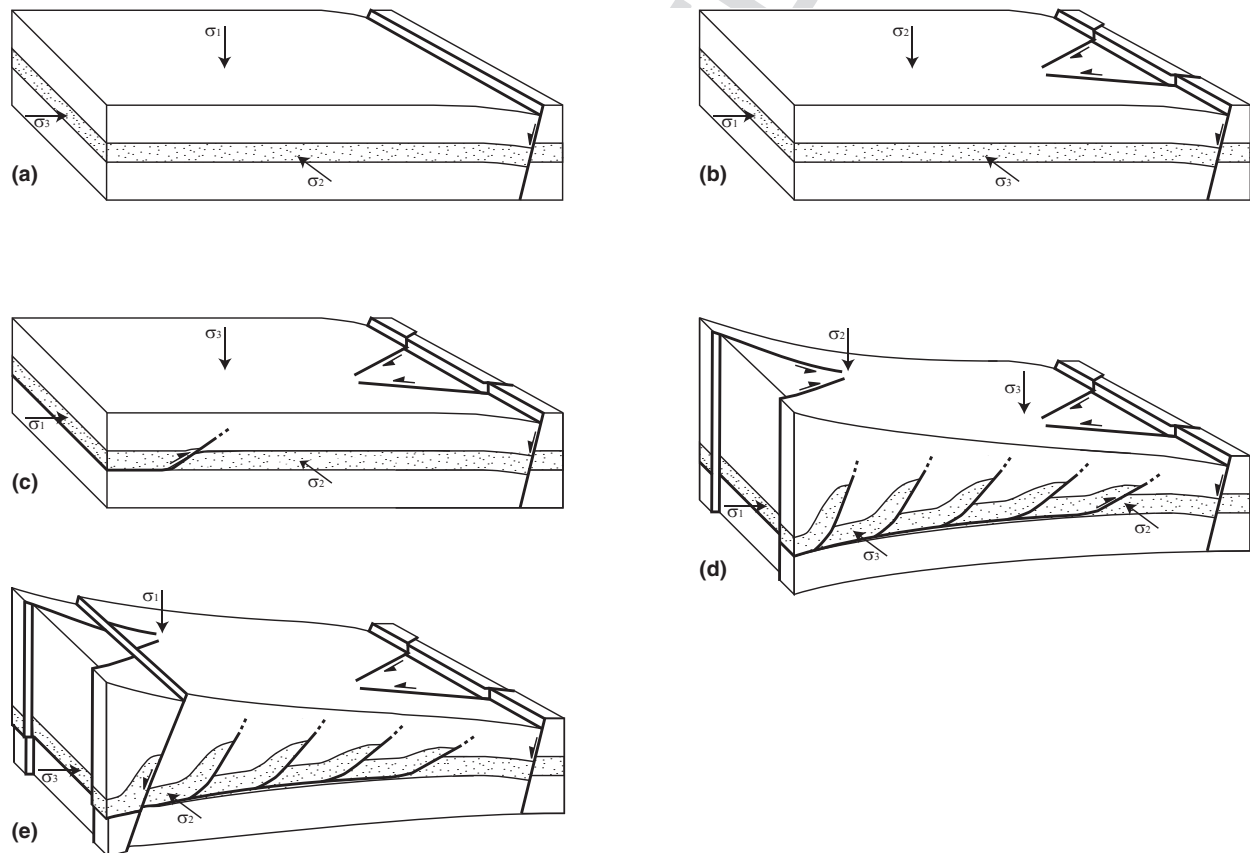5 Late-orogenic conjugate strike-slip faults are truncated by mainly SW-dipping post-orogenic normal

Fig. 5 The evolution of a stress system from basin development, through orogenesis, to post-orogenic extension. (a) Extension, with σ_1 vertical, creating normal faults. $P_f \geq \sigma_3$. (b) An increase in horizontal stresses causes σ_V to become σ_2, leading to the development of strike-slip faults. (c) Contractional deformation, with thrusts and folds developed as σ_V becomes σ_3. (d) Folding and thrusting cause an increase in overburden and a swap in the orientations of σ_3 and σ_2, with strike-slip faults developing. If σ_1 is at a high angle to the strike of the orogenic belt, then symmetrical conjugate strike-slip faults develop. There will be a tendency for a spatial and temporal partitioning of strain. (e) Orogenic collapse, with σ_1 vertical, caused either by crustal thickening or by a reduction of horizontal stresses at the end of orogenesis.
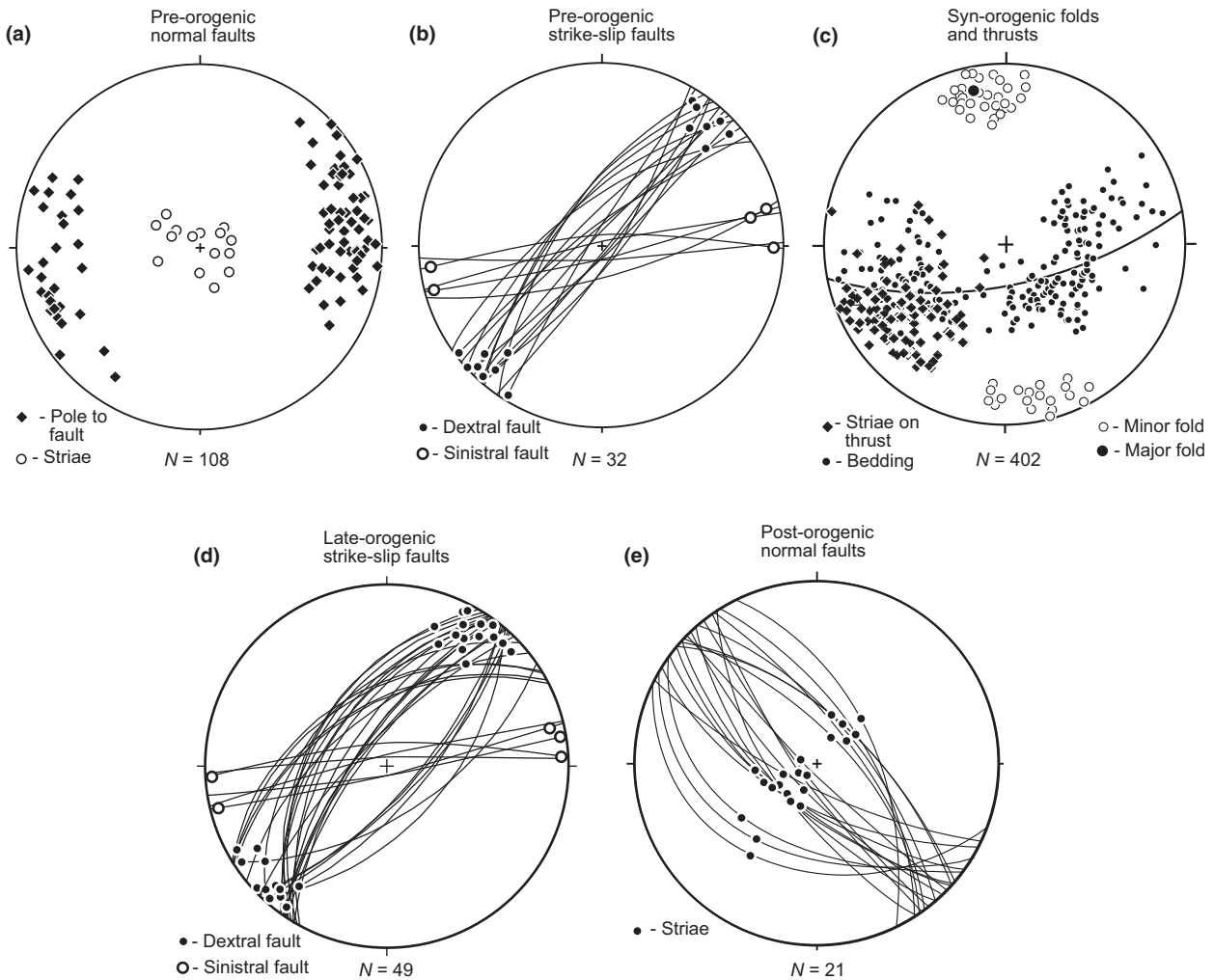
Fig. 6 Orientations of structures (equal-area projection, lower hemisphere) in the area to the SE of Spoleto. (a) Pre-orogenic normal faults. The mean extension direction is 081°. (b) Conjugate pre-orogenic strike-slip faults. The mean direction of contraction is 062°. (c) Orogenic contractional structures. The mean fold plunge is 18° towards 348°. The mean shortening direction is 069°. (d) Conjugate late-orogenic strike-slip faults. The mean direction of contraction is 061°. (e) Post-orogenic normal faults. The mean direction of extension is 049°.

faults (Fig. 4b). The change from contraction to extension from the Miocene led to the opening of the Tyrrhenian Sea in the innermost part of the mountain belt, that is, the westernmost orogenic provinces (Dewey *et al.*, 1989). Post-orogenic extension progressively migrated eastwards, so thrusts and related folds in the Umbria-Marche region, along with late-orogenic strike-slip faults, were overprinted by normal faults from the Early Pliocene (Lavecchia *et al.*, 1994; Calamita *et al.*, 2000). Slickensides on these post-orogenic normal faults indicate a mean 049°

extension direction with a local transtensional component (Figs. 5e, 6e and 7d). Most post-orogenic normal faults cropping out southeast of Spoleto (Fig. 4b) are consistent in orientation and kinematics with the normal faults that were responsible for the seismic events of: (i) Colfiorito (1997) to the north (Calamita *et al.*, 2000); (ii) L'Aquila (2009) to the southeast (Boncio *et al.*, 2012); and (iii) Amatrice (2016) to the east (Abbott and Scheiermeier, 2016). These post-orogenic normal faults may therefore still be tectonically active.

Model for the evolution of stress axes and fluid pressure

The examples presented here illustrate a more general relationship and evolution of stresses, P_f and deformation during burial and uplift (Fig. 8). Normal faults will tend to develop if $\sigma_1 = \sigma_V$, with vertical veins forming if $P_f > \sigma_h$ (Fig. 8a). As overburden decreases or the horizontal stresses increase, $\sigma_V = \sigma_2$, leading to the development of strike-slip faults (Fig. 8b). As overburden decreases or the horizontal (tectonic) stresses increase further, $\sigma_V = \sigma_3$, tending to produce overpressure,
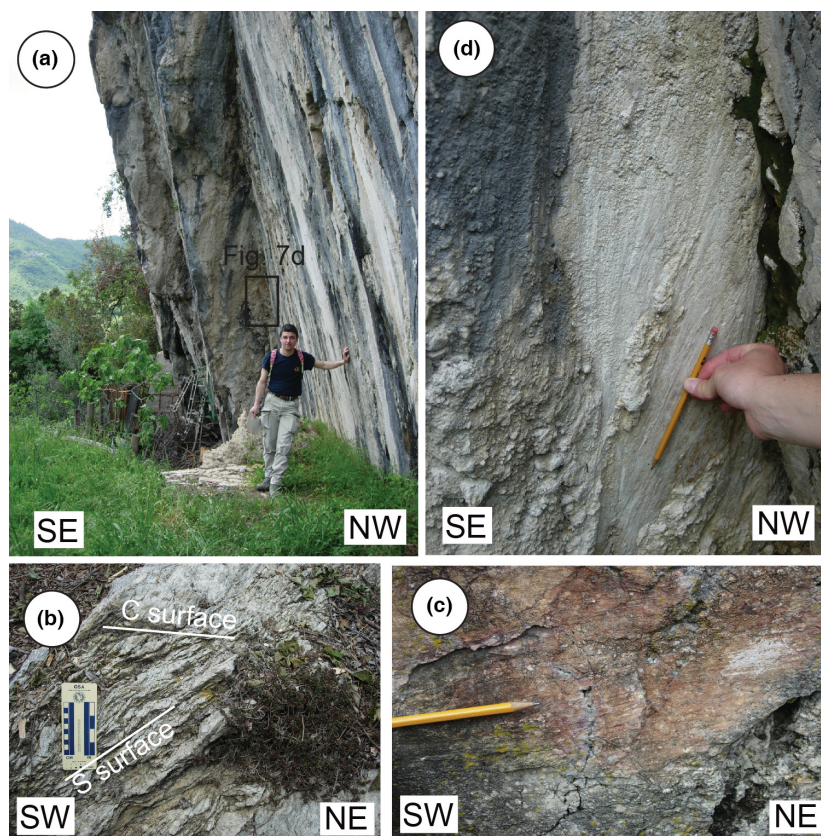
Fig. 7 Field examples of faults with different kinematic characters along the Valnerina Fault Zone near Schioppo (see location in Fig. 4b), illustrating the transition from late-orogenic strike-slip to post-orogenic extension. (a) The SW–NE-trending late-orogenic strike-slip Valnerina Fault produces a *c.* 10 m high scarp juxtaposing Jurassic limestones in the hangingwall with Oligocene marls in the footwall. (b) S/C fabrics developed within Oligocene marls in the footwall of the Valnerina Fault as seen from above. The intersection of the pressure solution cleavage (S) and shear surfaces (C) indicates dextral kinematics. (c) Slickensides and calcite fibres along the SW–NE-trending late-orogenic Valnerina Fault. Mechanical slickensides indicate a general strike-slip displacement, while steps in the calcite fibres indicate dextral kinematics. (d) Detail of Fig. 7a, showing a post-orogenic normal-fault surface that offsets the late-orogenic Valnerina strike-slip Fault with general dip-slip kinematics.

inversion and thrust faults (Fig. 8c). An increase in the horizontal stresses during inversion events can reduce porosity and therefore increase P_f (Turner and Williams, 2004). This sequence can occur in the opposite direction as σ_V increases, from thrust faults, through strike-slip faults, to normal faults (Fig. 8d–f). A phase of strike-slip faulting would tend to occur during inversion unless σ_1 and σ_3 swap over at the same value as σ_2, that is, if stresses are isotropic.

The evolution of stress axes and overpressure during progressive deformation is related to variations in the vertical and/or horizontal stresses, that is, variations in overburden and/or tectonic forces (e.g. Lavecchia and Pialli, 1981). σ_V will tend to decrease during crustal thinning or uplift and erosion, and increase during crustal thickening. For example, Harland and Bayly (1958) describe an 'orogenic sequence of regimes', with the increase in overburden and the relaxation of tectonic stresses after orogenesis causing strike-slip and eventually normal faulting.

Whilst P_f does not influence the relative magnitudes of the stress axes, the sequences of deformation illustrated in Fig. 8 will be promoted if

P_f is high enough to allow faulting to occur (e.g. Turner and Williams, 2004). Strike-slip faulting and inversion are less likely in unsealed units, where hydrostatic P_f is maintained. Inversion may therefore be partly related to the presence of sealing units and overpressure, which may explain the patchy development of Alpine inversion in the southern UK, where inversion structures are observed in areas with potential seal units (Fig. 1a).

Conclusions

The Mesozoic rocks of southern England are in the foreland to the Alpine deformation, whilst the Apennines of Umbria-Marche in Italy are part of an orogenic belt. Both areas, however, share the following features:

1 They demonstrate a deformation sequence from Mesozoic basin development (σ_1 vertical), to strike-slip deformation (σ_2 vertical), to Alpine contraction (σ_3 vertical), to strike-slip deformation (σ_2 vertical) and back to regional extension. The change between σ_1 being vertical during regional extension and σ_3 being vertical during regional contraction therefore involved a phase in which σ_2 was vertical, causing strike-slip faulting.

2 This deformation was promoted by high P_f, as indicated by the presence of veins.

3 Variations of stress axes occurred because of changes in overburden and/or tectonic forces. Reduction in overburden during uplift and erosion events probably caused overpressure to develop beneath sealing units, tending to promote the development of inversion structures (horizontal veins, thrusts and reverse-reactivated normal faults). Inversion structures may therefore be controlled by the presence of an effective seal unit, helping explain the patchy development of Alpine inversion structures in NW Europe.

These field examples, from different tectonic settings, suggest such behaviour is common in areas that have undergone single as well as multiple inversion.
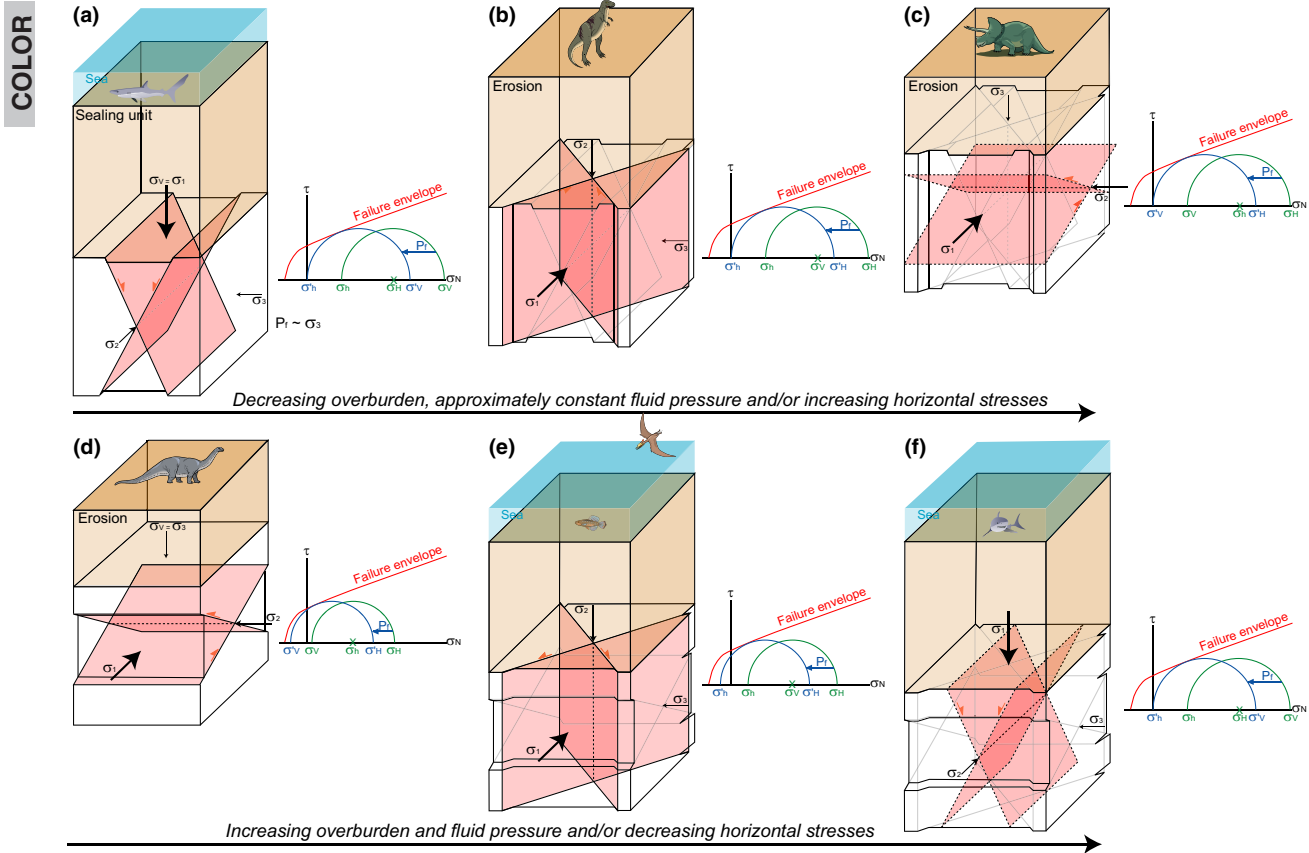
COLOR

Fig. 8 Schematic block diagrams and Mohr diagrams for stresses, fluid pressures and faulting. (a–c) Uplift and erosion (positive inversion) causes a decrease in overburden, but fluid pressure remains approximately constant beneath a sealing unit. (a) Normal faulting, with $\sigma_V = \sigma_1$. (b) The decrease in overburden and increase in horizontal stress causes $\sigma_V = \sigma_2$, promoting strike-slip faulting. (c) A further decrease in overburden and increase in horizontal stress causes $\sigma_V = \sigma_3$, promoting thrust faulting. (d–f) Subsidence and sedimentation (negative inversion) causes an increase in overburden and in fluid pressure. (d) Thrust faulting, with $\sigma_V = \sigma_3$. (e) The increase in overburden causes $\sigma_V = \sigma_2$, promoting strike-slip faulting. (f) A further increase in overburden causes $\sigma_V = \sigma_1$, promoting normal faulting.

References

Abbott, A. and Scheiermeier, Q., 2016. Italian scientists shocked by earthquake devastation. In a region known to be seismically active, destruction on this scale was still a surprise. *Nature*, **537**, 15–16.

Alfonsi, L., Funiciello, R. and Mattei, M., 1990. Strike-slip tectonics in the Sabina area. *Boll. Soc. Geol. Ital.*, **109**, 481–488.

Alvarez, W., 1990. Pattern of extensional faulting in pelagic carbonates of the Umbria-Marche Apennines of central Italy. *Geology*, **18**, 407–410.

Angelier, J., Colletta, B. and Anderson, R.E., 1985. Neogene paleostress changes in the Basin and Range: a case study at Hoover Dam, Nevada-Arizona. *Geol. Soc. Am. Bull.*, **96**, 347–361.

Barchi, M., 1991. Integration of a seismic profile with surface and subsurface geology in a cross-section through the Umbria-Marche Apennines. *Boll. Soc. Geol. Ital.*, **110**, 469–479.

Boncio, P., Galli, P., Naso, G. and Pizzi, A., 2012. Zoning surface rupture hazard along normal faults: Insight from the 2009 Mw 6.3 L'Aquila, Central Italy, earthquake and other global earthquakes. *Bull. Seismol. Soc. Am.*, **102**, 918–935.

Bowers, G.L., 2002. Detecting high overpressure. *Lead. Edge*, **???**, 174–177.

Butler, R.W.H., Tavarnelli, E. and Grasso, M., 2006. Preface: tectonic inversion and structural inheritance in mountain belts. *J. Struct. Geol.*, **28**, 1891–1892.

Calamita, F., Coppola, L., Deiana, G., Invernizzi, C. and Mastrovincenzo, S., 1987. Le associazioni strutturali di Genga e M. Rotondo: un motivo ricorrente nella thrust-belt umbro-marchigiana settentrionale. *Boll. Soc. Geol. Ital.*, **106**, 141–151.

Calamita, F., Cello, G., Deiana, G. and Paltrinieri, W., 1994. Structural styles, chronology rates of deformation and time-space relationships in the Umbria-Marche thrust system (Central Apennines, Italy). *Tectonics*, **13**, 873–881.

Calamita, F., Coltorti, M., Piccinini, D., Pierantoni, P.P., Pizzi, A., Ripepe, M., Scisciani, V. and Turco, E., 2000. Quaternary faults and seismicity in the Umbro-Marchean Apennines (Central Italy): evidence from the 1997 Colfiorito earthquake. *J. Geodynam.*, **29**, 245–264.

Chaput, M., Famin, V. and Michon, L., 2014. Deformation of basaltic shield volcanoes under cointrusive stress permutations. *J. Geophys. Res.*, **119**, 274–301.

Cobbold, P.R., Mourgues, R. and Boyd, K., 2004. Mechanism of thin-skinned detachment in the Amazon Fan: assessing the importance of fluid overpressure and hydrocarbon generation. *Mar. Petrol. Geol.*, **21**, 1013–1025.

Corcoran, D.V. and Doré, A.G., 2002. Depressurization of hydrocarbon-bearing reservoirs in exhumed basin settings: evidence from Atlantic margin and borderland basins. In: *Exhumation of the North Atlantic Margin: Timing, Mechanisms and Implications for Hydrocarbon Exploration* (A.G. Doré, J.A. Cartwright, M.S. Stoker, J.P. Turner and N. White, eds). *Geol. Soc. London. Spec. Publ.*, **196**, 457–483.

Dart, C.J., McClay, K. and Hollings, P.N., 1995. 3D analysis of inverted extensional fault systems, southern Bristol Channel basin, UK. In: *Basin Inversion* (J.G. Buchanan and P.G. Buchanan, eds). *Geol. Soc. London. Spec. Publ.*, **88**, 393–413.

Decandia, F.A., 1982. Geologia dei Monti di Spoleto (Prov. Di Perugia). *Boll. Soc. Geol. Ital.*, **101**, 291–315.

Decandia, F.A. and Giannini, E., 1977. Studi geologici nell'Appennino umbro-marchigiano. 3- Tettonica della zona di Spoleto. *Boll. Soc. Geol. Ital.*, **96**, 735–746.

Dewey, J.F., 1969. Structure and sequence in paratectonic British Caledonides. *Am. Assoc. Petrol. Geol. Mem.*, **12**, 309–335.

Dewey, J.F., Helman, M.L., Turco, E., Hutton, D.H.V. and Knott, S.D., 1989. Kinematics of the western Mediterranean. In: *Alpine Tectonics* (M.P. Coward, D. Dietrich and R.G. Park, eds.). *Geol. Soc. London. Spec. Publ.*, **45**, 265–283.

Doré, A.G. and Jensen, L.N., 1996. The impact of late Cenozoic uplift and erosion on hydrocarbon exploration: offshore Norway and some other uplifted basins. *Global Planet. Change*, **12**, 415–436.

Glen, R.A., Hancock, P.L. and Whittaker, A., 2005. Basin inversion by distributed deformation: the southern margin of the Bristol Channel Basin, England. *J. Struct. Geol.*, **27**, 2113–2134.

Harland, W.B. and Bayly, M.B., 1958. Tectonic regimes. *Geol. Mag.*, **95**, 89–104.

Hibsch, C., Jarrige, J.J., Cushing, E.M. and Mercier, J., 1995. Palaeostress analysis, a contribution to the understanding of basin tectonics and geodynamic evolution. Example of the Permian/Cenozoic tectonics of Great Britain and geodynamic implications in western Europe. *Tectonophysics*, **252**, 103–136.

Hubbert, M.K. and Rubey, W.W., 1959. Role of fluid pressure in mechanics of overthrust faulting. Parts I and II. *Geol. Soc. Am. Bull.*, **70**, 115–205.

Lahann, R.W. and Swarbrick, R.E., 2011. Overpressure generation by load transfer following shale framework weakening due to smectite diagenesis. *Geofluids*, **11**, 362–375.

Lake, S.D. and Karner, G.D., 1987. The structure and evolution of the Wessex Basin, southern England: an example of inversion tectonics. *Tectonophysics*, **137**, 347–378.

Lavecchia, G. and Pialli, G.P., 1981. Geodynamic evolution of Umbrian-Marchean Apennines: a suggestion. *Rend. Soc. Geol. Ital.*, **4**, 585–586.

Lavecchia, G., Brozzetti, F., Barchi, M., Meenichetti, M. and Keller, J.V.A., 1994. Seismotectonic zoning in east-central Italy deduced from an analysis of the Neogene to present deformations and related stress fields. *Geol. Soc. Am. Bull.*, **106**, 1107–1120.

Marshak, S., Geiser, P.A., Alvarez, W. and Engelder, T., 1982. Mesoscopic fault array of the northern Umbrian Apennine fold belt, Italy: geometry of conjugate shear by pressure-solution slip. *Geol. Soc. Am. Bull.*, **93**, 1013–1022.

Mazabraud, Y., Béthoux, N. and Delouis, B., 2013. Is earthquake activity along the French Atlantic margin favoured by local rheological contrasts? *Comp. Rend. Geosci.*, **345**, 373–382.

Nemčok, M., Gayer, R. and Miliorizos, M., 1995. Structural analysis of the inverted Bristol Channel Basin: implications for the geometry and timing of fracture porosity. In: *Basin Inversion* (J.G. Buchanan and P.G. Buchanan, eds). *Geol. Soc. London. Spec. Publ.*, **88**, 355–392.

Pace, P., Pasqui, V., Tavarnelli, E. and Calamita, F., 2016. Foreland-directed gravitational collapse along curved thrust fronts: insights from a minor thrust-related shear zone in the Umbria-Marche belt, central-northern Italy. *Geol. Mag.*, **???**, ???–???. doi: 10.1017/S0016756816000200. [4]

Peacock, D.C.P., 2001. The temporal relationship between joints and faults. *J. Struct. Geol.*, **23**, 329–341.

Peacock, D.C.P. and Sanderson, D.J., 1992. Effects of layering and anisotropy on fault geometry. *J. Geol. Soc. Lond.*, **149**, 793–802.

Peacock, D.C.P. and Sanderson, D.J., 1999. Deformation history and basin-controlling faults in the Mesozoic sedimentary rocks of the Somerset coast. *Proc. Geol. Assoc.*, **110**, 41–52.

Petroleum Exploration Society of Great Britain, 2000. *Structural Framework of the North Sea and Atlantic Margin.* Petroleum Exploration Society of Great Britain map. [5]

Plateaux, R., Bergerat, F., Béthoux, N., Villemin, T. and Gerbault, M., 2012. Implications of fracturing mechanisms and fluid pressure on earthquakes and fault slip data in the east Iceland rift zone. *Tectonophysics*, **581**, 19–34.

Rawnsley, K.D., Peacock, D.C.P., Rives, T. and Petit, J.-P., 1998. Jointing in the Mesozoic sediments around the Bristol Channel Basin. *J. Struct. Geol.*, **20**, 1641–1661.

Reches, Z., 1983. Faulting of rocks in three-dimensional strain fields: II theoretical analysis. *Tectonophysics*, **95**, 133–156. [6]

Rusciadelli, G., Viandante, M.G., Calamita, F. and Cook, A.C., 2005. Burial-exhumation history of the central Apennines (Italy), from the foreland to the chain building: thermochronological and geological data. *Terra Nova*, **17**, 560–572.

Satolli, S., Pace, P., Viandante, M.G. and Calamita, F., 2014. Lateral variations in tectonic style across cross-strike discontinuities: an example from the central Apennines belt (Italy). *Int. J. Earth Sci.*, **103**, 2301–2313.

Scisciani, V., Tavarnelli, E. and Calamita, F., 2001. Styles of tectonic inversion within syn-orogenic basins: examples from the Central Apennines, Italy. *Terra Nova*, **13**, 321–326.

Sibson, R.H., 2004. Controls on maximum fluid overpressure defining conditions for mesozonal mineralisation. *J. Struct. Geol.*, **26**, 1127–1136.

Sue, C., Le Gall, B. and Daoud, A.M., 2014. Stress field during early magmatism in the Ali Sabieh Dome, Djibouti, SE Afar rift. *J. Afr. Earth Sci.*, **97**, 56–66.

Swarbrick, R.E., Osborne, M.J. and Yardley, G.S., 2002. Comparison of overpressure magnitude resulting from the main generating mechanisms. In: *Pressure Regimes in Sedimentary Basins and their Prediction* (A.R. Huffman and G.L. Bowers, eds.). *Am. Assoc. Petrol. Geol. Mem.*, **76**, 1–12.

Tavarnelli, E., 1996. The effects of pre-existing normal faults on thrust ramp development: an example from the Northern Apennines, Italy. *Geol. Rund.*, **85**, 363–371.

Tavarnelli, E., 1997. Structural evolution of a foreland fold-and-thrust belt: the Umbria-Marche Apennines, Italy. *J. Struct. Geol.*, **19**, 523–534.

Tavarnelli, E., 1999. Normal faults in thrust sheets: pre-orogenic extension, post-orogenic extension, or both? *J. Struct. Geol.*, **21**, 1011–1018.

Tavarnelli, E. and Peacock, D.C.P., 1999. From extension to contraction in syn-orogenic foredeep basins: the Contessa section, Umbria-Marche Apennines, Italy. *Terra Nova*, **11**, 55–60.

Tesei, T., Collettini, C., Viti, C. and Barchi, M.R., 2013. Fault architecture and deformation mechanisms in exhumed analogues of seismogenic carbonate-bearing thrusts. *J. Struct. Geol.*, **55**, 1–15.

Tranos, M.D., 2013. The TR method: The use of slip preference to separate heterogeneous fault-slip data in compressional stress regimes. The surface rupture of the 1999 Chi-Chi Taiwan earthquake as a case study. *Tectonophysics*, **608**, 622–641.

Turner, J.P. and Williams, G.A., 2004. Sedimentary basin inversion and intra-plate shortening. *Earth-Sci. Rev.*, **65**, 277–304.

Underhill, J.R. and Patterson, S., 1998. Genesis of tectonic inversion structures: seismic evidence for the development of key structures along the Purbeck-Isle of Wight Disturbance. *J. Geol. Soc. Lond.*, **155**, 975–992.

Van Noten, K., Claes, H., Soete, J., Foubert, A., Özkul, M. and Swennen, R., 2013. Fracture networks and strike-slip deformation along reactivated normal faults in Quaternary travertine deposits, Denizli Basin, western Turkey. *Tectonophysics*, **588**, 154–170.

Vandycke, S., 2002. Palaeostress records in Cretaceous formations in NW Europe: extensional and strike-slip events in relations with Cretaceous-Tertiary inversion tectonics. *Tectonophysics*, **357**, 119–136.

Vandycke, S. and Bergerat, F., 2001. Brittle tectonic structures and palaeostress analysis in the Isle of Wight, Wessex basin, southern England. *J. Struct. Geol.*, **23**, 393–406.

Whittaker, A., 1972. The Watchet Fault - a post-Liassic transcurrent reverse fault. *Bull. Geol. Surv. G.B.*, **41**, 75–80.

Whittaker, A. and Green, G.W., 1983. *Geology of the Country Around Weston-super-Mare*. Mem. Geol. Surv. G.B., Sheet 279 and parts of 263 and 295.

Williams, G.D., Powell, C.M. and Cooper, M.A., 1989. Geometry and kinematics of inversion tectonics. In: *Inversion Tectonics* (M.A. Cooper and G.D. Williams, eds.). *Geol. Soc. London. Spec. Publ.*, **44**, 3–15.

Author Query Form

Dear Author,
During the copy-editing of your paper, the following queries arose. Please respond to these by marking up your proofs with the necessary changes/additions. Please write your answers on the query sheet if there is insufficient space on the page proofs. Please write clearly and follow the conventions shown on the attached corrections sheet. If returning the proof by fax do not write too close to the paper's edge. Please remember that illegible mark-ups may delay publication.
Many thanks for your assistance.

Query reference	Query	Remarks
1	**AUTHOR: Please confirm that given names (red) and surnames/family names (green) have been identified correctly.**	
2	**AUTHOR: Abbott and Scheirmeier, 2016 has been changed to Abbott and Scheiermeier, 2016 so that this citation matches the Reference List. Please confirm that this is correct.**	
3	**AUTHOR: Please provide the volume number for reference Bowers (2002).**	
4	**AUTHOR: Please provide the volume number, page range for reference Pace et al. (2016).**	
5	**AUTHOR: Please provide more details (if applicable) for reference Petroleum Exploration Society of Great Britain (2000).**	
6	**AUTHOR: Reches (1983) has not been cited in the text. Please indicate where it should be cited; or delete from the Reference List.**	
7	**AUTHOR: Please provide more details (if applicable) for reference Whittaker and Green (1983).**	